International Journal of Aerospace and Lightweight Structures
Vol. 1, No. 1 (2011) 23–46
© Research Publishing Services
DOI: 10.3850/S2010428611000079

LARGE DEFLECTION OF GEOMETRICALLY ASYMMETRIC METAL FOAM CORE SANDWICH BEAM TRANSVERSELY LOADED BY A FLAT PUNCH

QINGHUA QIN*, JIANXUN ZHANG, ZHENGJIN WANG and T. J. WANG[‡]

State Key Laboratory for Strength and Vibration of Mechanical Structures
Department of Engineering Mechanics Xi'an Jiaotong University
Xi'an, 710049, China
**qhqin@mail.xjtu.edu.cn*
† wangtj@mail.xjtu.edu.cn

Revised 1 September 2011
Accepted 4 September 2011

The objective of this work is to study the large deflection of geometrically asymmetric metal foam core sandwich beam under transverse loading by a fiat punch. A yield criterion is proposed for geometrically asymmetric metal foam core sandwich structures, and then analytical solution for the large deflection of a fully clamped slender sandwich beam is obtained, in which the interaction of bending and stretching induced by large deflection is considered. Also, finite element (FE) analysis is carried out. Comparisons of the analytical solution with numerical results are presented and good agreements are found. The effects of asymmetric factor, core strength and loading punch size on the structural response of asymmetric sandwich beam are discussed in detail. It is shown that the axial stretching induced by large deflection has significant effect on the load-carrying and energy absorption capacities of geometrically asymmetric sandwich structure, but the effect of asymmetry is negligible as the deflection is larger than the depth of the sandwich beam.

Keywords: Metal foam; geometrically asymmetric sandwich structure; yield criterion; asymmetric factor; large deflection.

1. Introduction

Lightweight sandwich structures are being widely used in a number of critical engineering, such as aircrafts, spacecrafts, vehicles, ships, high speed train carriages. The conventional sandwich structures have two identical face sheets in material and geometry. However, the face sheets may have different thickness and materials, and/or any combination of these for some special applications. The face sheets are generally made up of solid materials, such as steel, aluminum or fibre-reinforced composites and the cores are lightweight materials, including metal and polymer

[‡]Corresponding author.

foams, lattice and honeycomb structures, woven materials, egg-box [Ashby *et al.*, 2001; Deshpande and Fleck, 2001, 2003; Gibson and Ashby, 1997; Noor *et al.*, 1996; Queheillalt and Wadley, 2005; Sypeck DJ and Wadley, 2001; Wadley *et al.*, 2003; Xu *et al.*, 2010], etc.

In the past decades, investigations were devoted to analyzing the quasi-static deflection response and competing collapse modes of the simply supported sandwich beams with an aluminum foam core It has been recognized that sandwich beams fail by a number of competing mechanisms. Gibson and Ashby [1997] concluded the collapse mechanism maps of sandwich beams in bending to show the dependence of failure mode upon the geometry of beam and the strengths of the face sheets and core. Three-point bending experiments were carried out and metal foam core sandwich beams have several failure modes: face yield, indentation, core shear and face wrinkling, which were observed by Bart-Smith *et al.* [2001] and McCormack *et al.* [2001]. Also, they constructed the initial failure mode maps, which illustrate the dominant failure modes for practical design of sandwich structures. Subsequently, Bart-Smith *et al.* [2002] studied the retention of the load capacity of metal foam core sandwich beams in the presence of imperfections in four-point bending test. Moreover, Romanoff and Varsta [2006] obtained an analytical solution for the bending of a metal web-core sandwich beam under four-point-bending. Russell *et al.* [2011] studied the competing collapse mechanisms and structural response of simply supported and clamped carbon fiber sandwich beams with square honeycomb cores in three-point bending.

The aforementioned analyses are based on the assumption of small deflection, while there is little research on the large deflection response of sandwich structures with various boundary conditions, in which axial stretching induced by large deflection and the interaction of bending moment and axial force should be considered in analysis. Onat and Prager [1953] studied the limit analysis in which axial forces as well as bending moments were taken into account for the solid rectangular and I-type cross-sections, respectively. Haythornwaite [1957] experimentally and theoretically studied the effect of axial force on the large deflection response of fully clamped beam with solid rectangular cross-section subject to a transversely concentrated load. Moreover, Tagarielli *et al.* [2005, 2004] presented combined experimental and numerical investigations of the three-point bending of simply supported and clamped composite and metal foam core sandwich beams, respectively. They found that both the competing collapse modes of the simply supported are similar to those of fully clamped sandwich beams. Moreover, they developed an elastic model and an elastic–perfectly plastic model for fully clamped composite and metal foam core sandwich beam, respectively. The deformation is subdivided into three phases, i.e. elastic bending, transition and membrane phases.

The classical yield criterion may be highly accurate for the metal sandwich structure with thin and strong face sheets and a thick and weak core, but it becomes less accurate as the sandwich structure approaches the limit of monolithic solid one

Fleck and Deshpande [2004]. More recently, Qin and Wang [2008, 2009a] derived a new yield criterion for geometrically symmetric metal sandwich structures incorporating the effect of core strength and obtained an analytical solution for the large deflection of a slender symetric metal foam core sandwich beam with axial restraints under transverse loading by a flat punch. Based on the new yield criterion, Qin and Wang [2009b] and Qin *et al.* [2009] investigated the impulsive response of fully clamped symmetric metal sandwich beams by using the membrane factor method, in which interaction of bending and stretching is considered. Also, Qin and Wang [2007, 2011] investigated the impulsive response of a fully clamped circular metal foam core sandwich plate and the low-velocity impact response of a fully clamped metal foam core sandwich beam, respectively.

Up to now, very limited work was devoted to the asymmetric sandwich structures, e.g., Frostig *et al.* [1991] investigated the bending behavior of an asymmetric metal or composite sandwich beam with a flexible, foam-type core. The objective of this work is to study the large deflection of geometrically asymmetric sandwich beam with metal foam core under transverse loading by a flat punch. This paper is organized as follows. A yield criterion is proposed for geometrically asymmetric sandwich structures in Sec. 2. Analytical solutions for the large deflection of a fully clamped asymmetric metal foam core sandwich beam under transverse loading by a flat punch are derived in Sec. 3. In Sec. 4, finite element calculation is carried out and comparisons with analytical predictions are presented. Moreover, the effects of asymmetric factor, core strength and loading punch size on the structural response of the geometrically asymmetric sandwich beam are discussed in detail. The concluding remarks are presented in Sec. 5.

2. A Yield Criterion for the Geometrically Asymmetric Sandwich Structures

The yield criterion for symmetric metal sandwich structures considering the effect of core strength is proposed by Qin and Wang [2008, 2009a] which is not only accurate for the symmetric sandwich cross-section with thin and strong face sheets and a thick and weak foam core, but also for the symmetric sandwich one with a strong core. Also, it can reduce to the well-known yield criterion for the solid monolithic cross-section and the classical yield criterion for the sandwich cross-sections with a weak core, respectively Martin [1975]. Herein, a yield criterion is proposed for geometrically asymmetric sandwich structures incorporating the effect of core strength.

2.1. *Asymmetric factor*

Herein, we consider a geometrically asymmetric metal foam core sandwich beam with a rectangular cross-section and axial constraints, as shown in Fig. 1, in which b is the width of the cross-section. The top and bottom face sheets with thickness

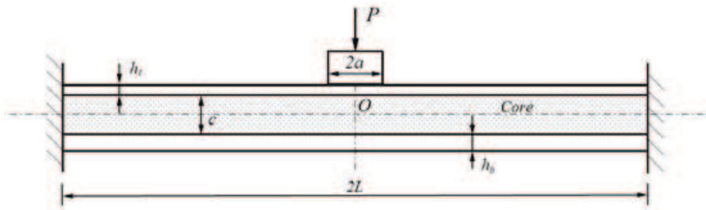

Fig. 1. Sketch of a fully clamped asymmetric sandwich beam transversely loaded by a flat punch.

h_t and h_b are perfectly bonded to the metal foam core with thickness c. It is assumed that the top and bottom face sheets obey the rigid-perfectly plastic law with the yield strength σ_f, and the metal foam core is modeled as a rigid-perfectly-plastic-locking (r-p-p-l) material with a plateau-stress σ_c and critical densification strain ε_D.

The asymmetric sandwich beam is transversely loaded at its midspan by a flat punch, as shown in Fig. 2. For the problem, the shear and axial forces and the bending moment should be considered simultaneously in analysis. Usually, the shear force is negligible compared with the bending moment and the axial force, particularly for structural response of the slender beams. In the case of large deflection, axial stretching and the interaction of bending and axial stretching are important and should be considered. Also, the core strength should be considered in analysis, especially for the sandwich structures with a strong metal foam core, since the metal foam core can offer higher stiffness and strength compared to the classical soft core, e.g., polymer foam.

Herein, we define a factor α to assess the asymmetry of the sandwich structures,

$$\alpha = h_t/h_b. \tag{2.1}$$

For the case of $0 < \alpha < 1$, the top face sheet is thinner than the bottom one. If $\alpha > 1$, the sandwich structure has a thicker top face sheet compared with the bottom one. If $\alpha = 1$, the sandwich structure is symmetrical. For the limit cases

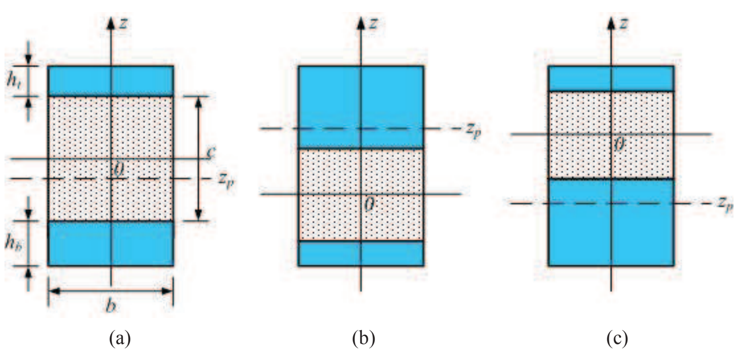

Fig. 2. Three cases of plastic neutral surfaces (a) in the core, (b) in the top face sheet and (c) in the bottom face sheet for asymmetric sandwich rectangular cross-sections in pure bending.

$\alpha \to 0$ or $\alpha \to \infty$, the sandwich structure reduces to a composite structure with two layers.

2.2. *Plastic neutral surface*

It is well known that the geometric and plastic neutral surfaces of the symmetric sandwich beam are coincident. However, the plastic neutral surface is different from the geometric surface for the asymmetric sandwich structure. Herein, we define z_p as the plastic neutral surface,

$$\int_{-\frac{c}{2}-h_b}^{z_p} \sigma(z)dz = \int_{z_p}^{\frac{c}{2}+h_t} \sigma(z)dz, \tag{2.2}$$

where $\sigma(z)$ is the yield strength of the material. Physically, we have from Eq. (2.2) that

$$z_p = \begin{cases} \dfrac{h_t - h_b}{2}\dfrac{\sigma_f}{\sigma_c}, & |z_p| \le \dfrac{c}{2} \\ \dfrac{h_t - h_b}{2} + \dfrac{c}{2}\left(1 - \dfrac{\sigma_c}{\sigma_f}\right), & \dfrac{c}{2} \le z_p \le \dfrac{c}{2} + h_t \\ \dfrac{h_t - h_b}{2} + \dfrac{c}{2}\left(\dfrac{\sigma_c}{\sigma_f} - 1\right), & -\left(\dfrac{c}{2} + h_b\right) \le z_p \le -\dfrac{c}{2}. \end{cases} \tag{2.3}$$

Moreover, if we define $\bar{\sigma} = \sigma_c/\sigma_f$ and $\bar{h} = \frac{h_t+h_b}{2c}$, then the location of plastic neutral surface can be expressed as

$$\delta = \frac{2\bar{h}(\alpha - 1)}{\bar{\sigma}(\alpha + 1)}. \tag{2.4}$$

It is seen that the plastic neutral surfaces located in the core as $|\delta| \le 1$, and in the top and bottom face sheets as $\delta > 1$ and $\delta < -1$, respectively.

2.3. *Yield criterion for the case of plastic neutral surface in the core ($-1 < \delta \le 1$)*

It is assumed that the sandwich cross-section has fully plastic stress distribution. The distributions of the strains and stresses in the asymmetric sandwich cross-section are shown in Fig. 3. The neutral surface is measured from the bottom face sheet, as shown in Fig. 3, which is denoted by $H = \zeta(c + h_t + h_b)$ with $\zeta = 0$, $[\zeta_0 = (z_p + h_b + c/2)/(h_t + h_b + c)]$ and 1 corresponding to fully plastic axial tension, bending and compression, respectively.

Here, we define that the value is positive when the moment turns clockwise. The resultants of the axial force N and the bending moment M for different values of ζ

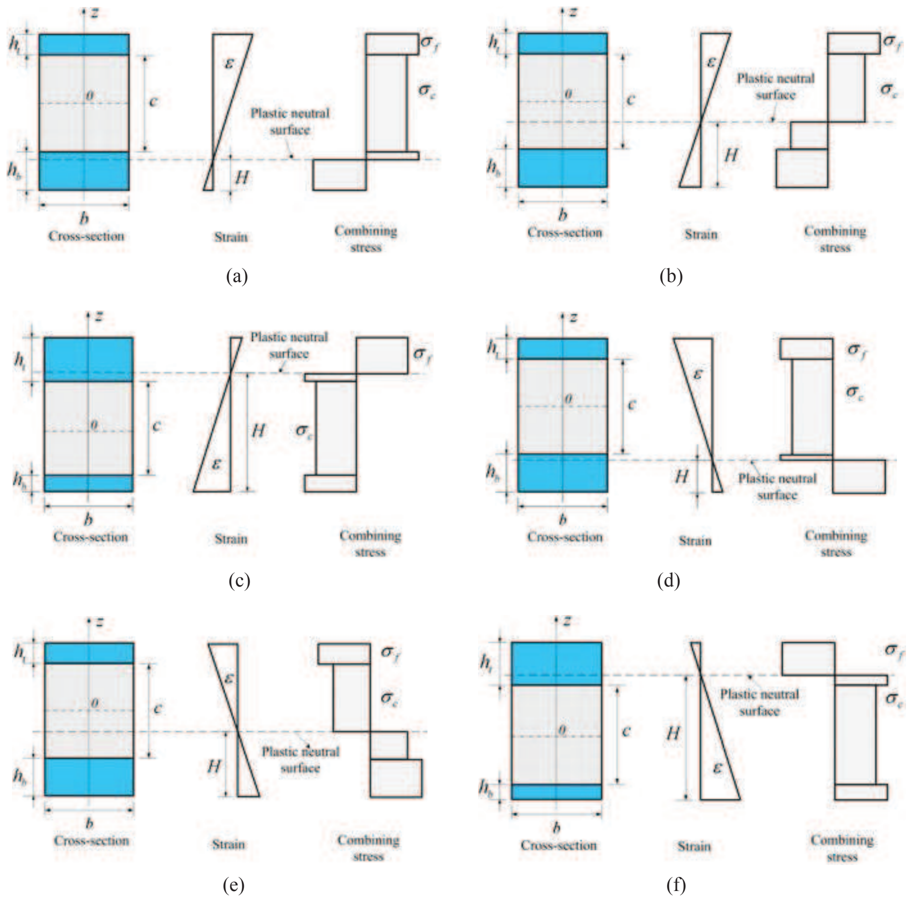

Fig. 3. Distributions of the strains and stresses on the cross-section of asymmetic sandwich beam under an axial force and a bending moment. (a) $M/M_p - C_1N/N_p \geq 0$, $0 \leq \zeta \leq h_b/(h_t + h_b + c)$, (b) $M/M_p - C_1N/N_p \geq 0$, $h_b/(h_t + h_b + c) \leq \zeta \leq (h_b + c)/(h_t + h_b + c)$, (c) $M/M_p - C_1N/N_p \geq 0$ and $(h_b + c)/(h_t + h_b + c) \leq \zeta \leq 1$, (d) $M/M_p - C_1N/N_p < 0$ and $0 \leq \zeta \leq h_b/(h_t + h_b + c)$, (e) $M/M_p - C_1N/N_p < 0$, $h_b/(h_t + h_b + c) \leq \zeta \leq (h_b + c)/(h_t + h_b + c)$, (f) $M/M_p - C_1N/N_p < 0$, $(h_b + c)/(h_t + h_b + c) \leq \zeta \leq 1$.

can be expressed as

$$N = \int_A \sigma dA = \begin{cases} \sigma_c bc + \sigma_f b[h_t + h_b - 2\zeta(c + h_t + h_b)], \quad 0 \leq \zeta \leq \dfrac{h_b}{c + h_t + h_b} \\ \sigma_f b(h_t - h_b) + \sigma_c b[c + 2h_b - 2\zeta(c + h_t + h_b)], \\ \dfrac{h_b}{c + h_t + h_b} \leq \zeta \leq \dfrac{c + h_b}{c + h_t + h_b} \\ -\sigma_c bc - \sigma_f b[h_t + h_b - 2(1 - \zeta)(c + h_t + h_b)], \\ \dfrac{c + h_b}{c + h_t + h_b} \leq \zeta \leq 1 \end{cases} \tag{2.5}$$

and

$$M = \int_A \sigma z dA = \begin{cases} \sigma_f b(c+h_b+h_t) \\ \quad \times \left[\dfrac{h_t-h_b}{2} - z_p - \zeta^2(c+h_t+h_b) + \zeta(c+2z_p+2h_b)\right] \\ \quad + (\sigma_f-\sigma_c)bcz_p, 0 \le \zeta \le \dfrac{h_b}{c+h_b+h_t} \\ \dfrac{\sigma_f b}{2}[(c+2z_p+h_b)h_b + (c-2z_p+h_t)h_t] \\ \quad + \dfrac{\sigma_c b}{4}\{c^2+4z_p^2 - [c+2z_p+2h_b-2\zeta(c+h_b+h_t)]^2\}, \\ \dfrac{h_b}{c+h_b+h_t} \le \zeta \le \dfrac{c+h_b}{c+h_b+h_t} \sigma_f b(c+h_b+h_t) \\ \quad \times \left[\dfrac{h_b-h_t}{2} + z_p - (1-\zeta)^2(c+h_b+h_t) + (1-\zeta)(c+h_b+h_t)\right] \\ \quad + (\sigma_c-\sigma_f)bcz_p, \dfrac{c+h_b}{c+h_b+h_t} \le \zeta \le 1 \end{cases} \tag{2.6}$$

in Figs. 3(a)–3(c). For the limit cases of $\zeta = 0$ and ζ_0, we respectively obtain

$$N_p = \sigma_c bc + \sigma_f b(h_t + h_b) \tag{2.7}$$

and

$$M_p = \frac{1}{2}\sigma_f b[(c-2z_p+h_t)h_t + (c+2z_p+h_b)h_b] + \frac{1}{4}\sigma_c b(c^2+4z_p^2) \tag{2.8}$$

Thus, it follows from Eqs. (2.7) and (2.8) that

$$\frac{N_p c}{M_p} = \frac{4A_1\bar{\sigma}}{\bar{\sigma}+2\bar{h}}, \tag{2.9}$$

where

$A_1 = (\bar{\sigma}+2\bar{h})^2(\alpha+1)^2/E_1$
$E_1 = 4\bar{\sigma}\bar{h}[(\alpha+1)^2 + 2(1+\alpha^2)\bar{h}] + \bar{\sigma}^2(\alpha+1)^2 - 4(\alpha-1)^2\bar{h}^2$

From Eqs. (2.5) to (2.9), we have

$$\frac{N}{N_p} = \begin{cases} 1 - \dfrac{2(1+2\bar{h})}{\bar{\sigma}+2\bar{h}}\zeta, \quad 0 \le \zeta \le \dfrac{2\bar{h}}{(\alpha+1)(1+2\bar{h})} \\ \dfrac{2(\alpha-1)\bar{h} + \bar{\sigma}[\alpha+1+4\bar{h}-2\zeta(\alpha+1)(1+2\bar{h})]}{(\alpha+1)(\bar{\sigma}+2\bar{h})}, \\ \dfrac{2\bar{h}}{(\alpha+1)(1+2\bar{h})} \le \zeta \le \dfrac{\alpha+1+2\bar{h}}{(\alpha+1)(1+2\bar{h})} \\ -1 + \dfrac{2(1+2\bar{h})}{\bar{\sigma}+2\bar{h}}(1-\zeta), \quad \dfrac{\alpha+1+2\bar{h}}{(\alpha+1)(1+2\bar{h})} \le \zeta \le 1 \end{cases} \tag{2.10}$$

and

$$\frac{M}{M_p}=\begin{cases}\dfrac{4(\alpha+1)(1+2h)\zeta[(1+\alpha)\bar{\sigma}+2(2\bar{\sigma}+\alpha-1)\bar{h}]}{4\bar{\sigma}\bar{h}[(\alpha+1)^2+2(1+\alpha^2)\bar{h}]+\bar{\sigma}^2(\alpha+1)^2-4(\alpha-1)^2\bar{h}^2}\\ \quad+\dfrac{8(\alpha^2-1)(\bar{\sigma}-1)\bar{h}^2-4\zeta^2\bar{\sigma}(\alpha+1)^2(1+2\bar{h})^2}{4\bar{\sigma}\bar{h}[(\alpha+1)^2+2(1+\alpha^2)\bar{h}]+\bar{\sigma}^2(\alpha+1)^2-4(\alpha-1)^2\bar{h}^2},\\ \quad 0\le\zeta\le\dfrac{2\bar{h}}{(\alpha+1)(1+2\bar{h})}\\ 1-\dfrac{[\bar{\sigma}(\alpha+1)+2(2\bar{\sigma}+\alpha-1)\bar{h}-2\zeta\bar{\sigma}(\alpha+1)(1+2\bar{h})]^2}{4\bar{\sigma}\bar{h}[(\alpha+1)^2+2(1+\alpha^2)\bar{h}]+\bar{\sigma}^2(\alpha+1)^2-4(\alpha-1)^2\bar{h}^2},\\ \quad\dfrac{2\bar{h}}{(\alpha+1)(1+2\bar{h})}\le\zeta\le\dfrac{\alpha+1+2\bar{h}}{(\alpha+1)(1+2\bar{h})}\\ \quad\dfrac{4(\alpha+1)(1+2\bar{h})(1-\zeta)[(1+\alpha)\bar{\sigma}+2(2\alpha\bar{\sigma}-\alpha+1)\bar{h}]}{4\bar{\sigma}\bar{h}[(\alpha+1)^2+2(1+\alpha^2)\bar{h}]+\bar{\sigma}^2(\alpha+1)^2-4(\alpha-1)^2\bar{h}^2}\\ +\dfrac{8(1-\alpha^2)(\bar{\sigma}-1)\bar{h}^2-4(1-\zeta)^2\bar{\sigma}(1+\alpha)^2(1+2\bar{h})^2}{4\bar{\sigma}\bar{h}[(\alpha+1)^2+2(1+\alpha^2)\bar{h}]+\bar{\sigma}^2(\alpha+1)^2-4(\alpha-1)^2\bar{h}^2},\\ \quad\dfrac{\alpha+1+2\bar{h}}{(\alpha+1)(1+2\bar{h})}\le\zeta\le 1.\end{cases}\tag{2.11}$$

Similarly, we can obtain the expressions of N/N_p and M/M_p for the case of $M/M_p - C_1N/N_p < 0$, where $C_1 = 8(\alpha^2-1)(\bar{\sigma}-1)\bar{h}^2/E_1$

Eliminating the parameter ζ from Eqs. (2.10) and (2.11) and using the well-known Tresca yield criterion, we have the following yield criterion for the geometrically asymmetric sandwich section when $m - C_1 n \ge 0$

$$\begin{cases}m+A_1\bar{\sigma}(n+1)^2-B_1(n+1)+C_1=0, & -1\le n\le n_1\\ m+A_1n^2=1, & n_1\le n\le n_2\\ m+A_1\bar{\sigma}(n-1)^2+D_1(n-1)-C_1=0, & n_2\le n\le 1\end{cases}\tag{2.12a}$$

where

$m = M/M_p$

$n = N/N_p$

$n_1 = \frac{2(\alpha-1)\bar{h}-\bar{\sigma}(\alpha+1)}{(\alpha+1)(\bar{\sigma}+2\bar{h})}$

$n_2 = \frac{2(\alpha-1)\bar{h}+\bar{\sigma}(\alpha+1)}{(\alpha+1)(\bar{\sigma}+2\bar{h})}$

$B_1 = 2(\alpha+1)(\bar{\sigma}+2\bar{h})[(1+\alpha)\bar{\sigma}+2(2\alpha\bar{\sigma}-\alpha+1)\bar{h}]/E_1$

$D_1 = 2(\alpha+1)(\bar{\sigma}+2\bar{h})[(1+\alpha)\bar{\sigma}+2(2\bar{\sigma}+\alpha-1)\bar{h}]/E_1$

When $m - C_1 n < 0$, we obtain

$$\begin{cases} m - A_1\bar{\sigma}(n+1)^2 + D_1(n+1) + C_1 = 0, & -1 \le n \le -n_2 \\ m - A_1 n^2 = -1, & -n_2 \le n \le -n_1 \\ m - A_1\bar{\sigma}(n-1)^2 - B_1(n-1) - C_1 = 0, & -n_1 \le n \le 1. \end{cases} \tag{2.12b}$$

It is readily seen that if the asymmetric factor $\alpha = 1$, then the yield criterion Eq. (2.12a) or (2.12b) reduces to the following one for symmetric sandwich structures [Qin and Wang, 2009a]

$$\begin{cases} |m| + \dfrac{(\bar{\sigma}+2\bar{h})^2}{4\bar{\sigma}\bar{h}(1+\bar{h})+\bar{\sigma}^2}n^2 = 1, & 0 \le |n| \le \dfrac{\bar{\sigma}}{\bar{\sigma}+2\bar{h}} \\ |m| + \dfrac{(\bar{\sigma}+2\bar{h})[(\bar{\sigma}+2\bar{h})|n| + 2\bar{h} - \bar{\sigma} + 2](|n|-1)}{4\bar{h}(1+\bar{h})+\bar{\sigma}}, & \dfrac{\bar{\sigma}}{\bar{\sigma}+2\bar{h}} \le |n| \le 1. \end{cases} \tag{2.13}$$

2.4. *Yield criterion for the case of plastic neutral surfaces out of the core ($\delta < -1$ and $\delta > 1$)*

Employing the same procedure as Sec. 2.3, we have the yield criterion of the asymmetric sandwich section for the case of plastic neutral surface in the top face sheet. When $m - F_2 n \ge 0$

$$\begin{cases} m + A_2 n^2 = 1, & -1 \le n \le n_1 \\ m + (B_2 + C_2 n)^2/[(\alpha+1)\bar{\sigma}H_2] - D_2 = 0, & n_1 \le n \le n_2 \\ m + (E_2 n + F_2)(n-1) - G_2 = 0, & n_2 \le n \le 1. \end{cases} \tag{2.14a}$$

When $m - F_2 n < 0$, we have

$$\begin{cases} m - (E_2 n - F_2)(n+1) + G_2 = 0, & -1 \le n \le -n_2 \\ m - (B_2 - C_2 n)^2/[(\alpha+1)\bar{\sigma}H_2] + D_2 = 0, & -n_2 \le n \le -n_1 \\ m - A_2 n^2 = -1, & -n_1 \le n \le 1, \end{cases} \tag{2.14b}$$

where

$A_2 = (\alpha+1)(\bar{\sigma}+2\bar{h})^2/H_2$
$B_2 = (\bar{\sigma}-1)[2(\alpha-1)\bar{h} - \bar{\sigma}(\alpha+1)]$
$C_2 = (\alpha+1)(\bar{\sigma}+2\bar{h})$
$D_2 = \{4\bar{h}[4\alpha\bar{h} + (\alpha+1)(\alpha\bar{\sigma} + 2 - \bar{\sigma})] + \bar{\sigma}(\alpha+1)^2 + \bar{\sigma}[2(\alpha-1)\bar{h} + (\alpha+1)(1-\bar{\sigma})]^2\}/[(\alpha+1)H_2]E_2 = (\alpha+1)(\bar{\sigma}+2\bar{h})^2/H_2$
$F_2 = (\alpha+1)(\bar{\sigma}+2\bar{h})(2\bar{h} - 3\bar{\sigma} + 4)/H_2$
$G_2 = 2(\bar{\sigma}-1)[\bar{\sigma}(\alpha+1) + 4\bar{h}]/H_2$
$H_2 = 4\bar{h}[(\alpha+1)\bar{h} + (\alpha-1)\bar{\sigma} + 2] - (\alpha+1)(\bar{\sigma}-1)^2 + (\alpha+1).$

Replacing the α and m in Eqs. (2.14a) and (2.14b) by $1/\alpha$ and $-m$, we can easily obtain the yield criterion for the case of plastic neutral surface in the bottom face sheet.

The predicted yield surfaces for the geometrically asymmetric metal sandwich cross-sections are shown in Fig. 4. It is clear that the present yield criterion is

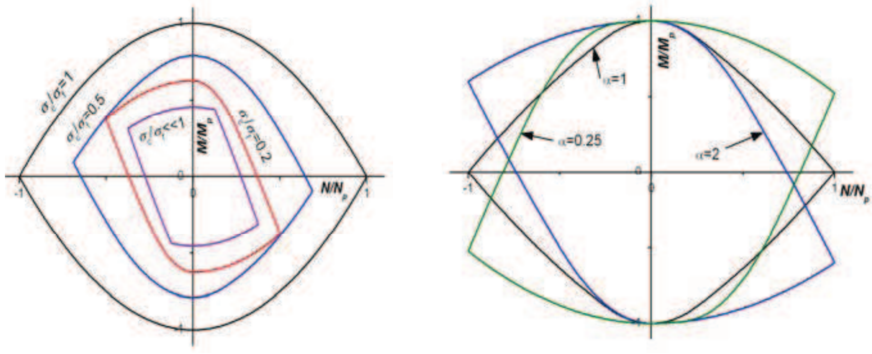

(a) (b)

Fig. 4. Yield loci for the asymmetic sandwich rectangular cross-sections with (a) core strength ($\alpha = 2, \bar{h} = 0.3$) and (b) asymmetric factor ($\bar{\sigma} = 0.2, \bar{h} = 0.3$).

valid for the asymmetric metal sandwich cross-sections with different core strength and geometries and can reduce to the yield criterion for the symmetric sandwich cross-sections [Qin and Wang, 2009a]. In what follows, the yield criterion would be employed to derive the analytical solutions for the large deflection of fully clamped geometrically asymmetric sandwich beams with a metal foam core, in which the interaction of bending and stretching is considered.

3. Analytical Solution for Large Deflection of Fully Clamped Asymmetric Sandwich Beam

Herein, we consider a geometrically asymmetric metal foam core sandwich beam with fully clamped boundary condition under transverse loading by a flat punch as shown in Fig. 1. This is a slender beam with the span $2L$ and the loading punch width $2a$. It is assumed that the slender asymmetric sandwich beam deforms in a global manner without local denting beneath the central punch. Thus, the sandwich cross-sections keep the original shape and the transverse deflection profile is the same as that of fully clamped rigid-perfectly plastic solid beam under transverse loading by a flat punch.

If the bottom face sheet has the maximum transverse deflection W under load P, then the left-hand portion (L-a) of the sandwich beam have a total extension e

$$e = e_1 + e_2, \tag{3.1}$$

where e_1 and e_2 are the axial extensions concentrated at the ends of the left-hand portion, as shown in Fig. 5(a). The total elongation of left-hand part of the sandwich beam is

$$e \approx \frac{W_0^2}{2(L-a)}. \tag{3.2}$$

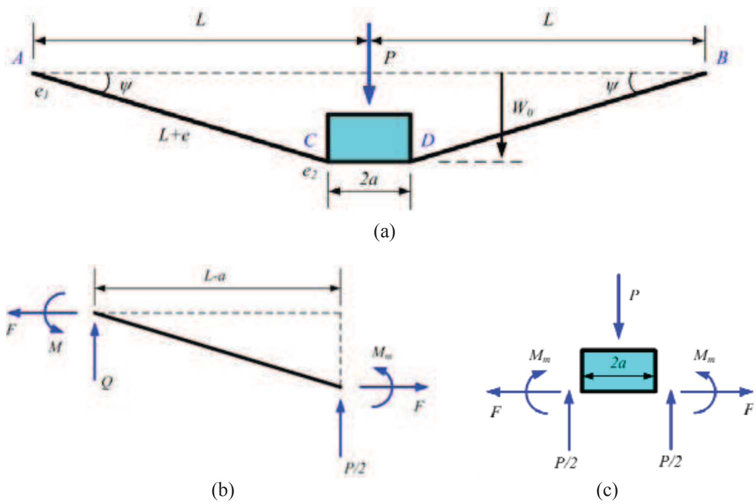

Fig. 5. Overall deformation pattern of the neutral surface of the fully clamped asymmetric sandwich beam with a metal foam core transversely loaded by a flat punch. (a) Transverse deflection pro?le, (b) forces and moments on the cross-section and (c) forces and moments on the punch.

The angular rotation, as shown in Fig. 5(a), is

$$\psi \approx \frac{W_0}{L-a}. \tag{3.3}$$

The moment equilibrium equation for the sandwich beam, as shown in Fig. 5(b), may be written as

$$2(M + M_m) - P(L-a) + 2FW_0 = 0. \tag{3.4}$$

where $F \approx N$ for moderate deflection. When $N = 0$, $M = M_p$ and $W_0 = 0$, the global deformation of the sandwich beam occurs, and a static collapse load $\bar{P}_c$ can be determined from Eq. (3.4)

$$\bar{P}_c = \frac{4M_p}{L-a}. \tag{3.5}$$

3.1. *The plastic neutral surface located in the core* $(-1 < \delta \le 1)$

According to the associated flow rules of yield criteria Eqs. (2.12a) and (2.12b) for asymmetric sandwich beam, we obtain the following normality relation at the fully clamped ends and the points adjacent to the central punch of the sandwich beam, respectively

$$\frac{\dot{e}_1}{\dot{\psi}} = \begin{cases} \dfrac{\bar{\sigma} + 2\bar{h}}{2\bar{\sigma}} cn, & 0 \le n \le n_2 \\ \dfrac{c}{2}[(\bar{\sigma} + 2\bar{h})(n-1) + 1] + \dfrac{(2\bar{\sigma} + \alpha - 1)c\bar{h}}{(\alpha+1)\bar{\sigma}}, & n_2 \le n \le 1 \end{cases} \tag{3.6a}$$

and

$$\frac{\dot{e}_2}{\dot{\psi}} = \begin{cases} \dfrac{\bar{\sigma}+2\bar{h}}{2\bar{\sigma}}cn, & 0 \le n \le -n_1 \\ \dfrac{c}{2}[(\bar{\sigma}+2\bar{h})(n-1)+1] + \dfrac{(2\alpha\bar{\sigma}-\alpha+1)c\bar{h}}{(\alpha+1)\bar{\sigma}}, & -n_1 \le n \le 1. \end{cases} \tag{3.6b}$$

Substituting Eqs. (3.1)–(3.3) into Eqs. (3.6a) and (3.6b), we have the relationship between the deflection W and non-dimensional axial force n. Two cases of the plastic neutral surface in the core, i.e. $-1 \le \delta \le 0$ and $0 < \delta \le 1$ are considered.

$$W_0^* = \frac{W_0}{c+h_t+h_b}$$
$$= \begin{cases} \dfrac{\bar{\sigma}+2\bar{h}}{\bar{\sigma}(1+2\bar{h})}n, & 0 \le n \le n_2 \\ \dfrac{(\bar{\sigma}+2\bar{h})(\bar{\sigma}+1)}{2\bar{\sigma}(1+2\bar{h})}n - \dfrac{\bar{\sigma}+2\bar{h}-1}{2(1+2\bar{h})} + \dfrac{(2\bar{\sigma}+\alpha-1)\bar{h}}{(\alpha+1)\bar{\sigma}(1+2\bar{h})}, & \\ n_2 \le n \le -n_1 & \\ \dfrac{(\bar{\sigma}+2\bar{h})(n-1)}{1+2\bar{h}} + 1, & -n_1 \le n \le 1 \end{cases} \tag{3.7a}$$

for the case of $-1 \le \delta \le 0$, and

$$W_0^* = \begin{cases} \dfrac{(\bar{\sigma}+2\bar{h})}{\bar{\sigma}(1+2\bar{h})}n, & 0 \le n \le -n_1 \\ \dfrac{(\bar{\sigma}+2\bar{h})(\bar{\sigma}+1)}{2\bar{\sigma}(1+2\bar{h})}n - \dfrac{\bar{\sigma}+2\bar{h}-1}{2(1+2\bar{h})} + \dfrac{(2\alpha\bar{\sigma}-\alpha+1)\bar{h}}{(\alpha+1)\bar{\sigma}(1+2\bar{h})}, & -n_1 \le n \le n_2 \\ \dfrac{(\bar{\sigma}+2\bar{h})(n-1)}{1+2\bar{h}} + 1, & n_2 \le n \le 1, \end{cases} \tag{3.7b}$$

for the case of $0 < \delta \le 1$ From Eqs. (2.12a and 2.12b), (3.4) and (3.7a) and (3.7b), we have

$$\frac{P}{P_c} = \begin{cases} \dfrac{1}{1-\bar{a}}\left[\dfrac{A_1\bar{\sigma}^2(1+2\bar{h})^2}{(\bar{\sigma}+2\bar{h})^2}W_0^{*2}+1\right], \quad 0 \le W_0^* \le \dfrac{(\bar{\sigma}+2\bar{h})n_2}{\bar{\sigma}(1+2\bar{h})} \\ \dfrac{1}{2(1-\bar{a})}\left[\dfrac{4A_1\bar{\sigma}^2(1+2\bar{h})^2}{(\bar{\sigma}+2\bar{h})^2(\bar{\sigma}+1)}W_0^{*2} - \dfrac{8K_3A_1\bar{\sigma}^2(1+2\bar{h})^2}{(\bar{\sigma}+2\bar{h})^2(\bar{\sigma}+1)}W_0^*\right] \\ \quad + \dfrac{1}{2(1-\bar{a})}\left[\dfrac{4K_1^2A_1\bar{\sigma}^2(1+2\bar{h})^2}{(\bar{\sigma}+2\bar{h})^2(\bar{\sigma}+1)} + C_1 + D_1 - A_1\bar{\sigma} + 1\right], \\ \dfrac{(\bar{\sigma}+2\bar{h})n_2}{\bar{\sigma}(1+2\bar{h})} \le W_0^* \le 1 - \dfrac{(\bar{\sigma}+2\bar{h})(1+n_1)}{1+2\bar{h}} \\ \dfrac{1}{1-\bar{a}}\left[\dfrac{A_1\bar{\sigma}(1+2\bar{h})^2}{(\bar{\sigma}+2\bar{h})^2}W_0^{*2} + \dfrac{2A_1\bar{\sigma}(1+2\bar{h})(\bar{\sigma}-1)}{(\bar{\sigma}+2\bar{h})^2}W_0^* + \dfrac{A_1\bar{\sigma}(1+2\bar{h})^2}{(\bar{\sigma}+2\bar{h})^2}\right], \\ 1 - \dfrac{(\bar{\sigma}+2\bar{h})(1+n_1)}{1+2\bar{h}} \le W_0^* \le 1. \end{cases} \tag{3.8a}$$

for the case of $-1 \le \delta \le 0$, and

$$\frac{P}{P_c} = \begin{cases} \frac{1}{1-\bar{a}}\left[\frac{A_1\bar{\sigma}^2(1+2\bar{h})^2}{(\bar{\sigma}+2\bar{h})^2}W_0^{*2}+1\right], \quad 0 \le W_0^* \le -\frac{(\bar{\sigma}+2\bar{h})n_1}{\bar{\sigma}(1+2\bar{h})} \\ \frac{1}{2(1-\bar{a})}\left[\frac{4A_1\bar{\sigma}^2(1+2\bar{h})^2}{(\bar{\sigma}+2\bar{h})^2(\bar{\sigma}+1)}W_0^{*2} - \frac{8K_1A_1\bar{\sigma}^2(1+2\bar{h})^2}{(\bar{\sigma}+2\bar{h})^2(\bar{\sigma}+1)}W_0^*\right] \\ +\frac{1}{2(1-\bar{a})}\left[\frac{4K_2^2A_1\bar{\sigma}^2(1+2\bar{h})^2}{(\bar{\sigma}+2\bar{h})^2(\bar{\sigma}+1)} + B_1 - C_1 - A_1\bar{\sigma} + 1\right], \\ -\frac{(\bar{\sigma}+2\bar{h})n_1}{\bar{\sigma}(1+2\bar{h})} \le W_0^* \le 1 - \frac{(\bar{\sigma}+2\bar{h})(1-n_2)}{1+2\bar{h}} \\ \frac{1}{1-\bar{a}}\left[\frac{A_1\bar{\sigma}(1+2\bar{h})^2}{(\bar{\sigma}+2\bar{h})^2}W_0^{*2} + \frac{2A_1\bar{\sigma}(1+2\bar{h})(\bar{\sigma}-1)}{(\bar{\sigma}+2\bar{h})^2}W_0^* + \frac{A_1\bar{\sigma}(1+2\bar{h})^2}{(\bar{\sigma}+2\bar{h})^2}\right], \\ 1 - \frac{(\bar{\sigma}+2\bar{h})(1-n_2)}{1+2\bar{h}} \le W_0^* \le 1 \end{cases} \tag{3.8b}$$

for the case of $0 < \delta \le 1$, in which

$P_c = \frac{4M_p}{L}$

$\bar{a} = a/L$

$K_1 = \frac{(1-\bar{\sigma})[(1+\alpha)\bar{\sigma}-2\bar{h}(1-\alpha)]}{2(1+2\bar{h})(1+\alpha)\bar{\sigma}}$

$K_2 = \frac{1-\bar{\sigma}-2\bar{h}}{2(1+2\bar{h})} + \frac{(2\alpha\bar{\sigma}-\alpha+1)\bar{h}}{(1+\alpha)\bar{\sigma}(1+2\bar{h})}$

It should be noted that in the case of $W_0^* \ge 1$, $n = 1$, the asymmetric sandwich beam is in a membrane state and behaves like a stretched plastic string. Such that

$$\frac{P}{P_c} = \frac{2A_1\bar{\sigma}\left(1+2\bar{h}\right)}{(1-\bar{a})\left(\bar{\sigma}+2\bar{h}\right)}W_0^* \tag{3.8c}$$

Let the asymmetric factor $\alpha = 1$, then Eqs. (3.8a)–(3.8c) reduce to the following solutions for symmetric sandwich beam transversely loaded by a flat punch at midspan [Qin and Wang, 2009a]

$$\frac{P}{P_c} = \begin{cases} \frac{1}{1-\bar{a}}\left[\frac{\bar{\sigma}(1+2\bar{h})^2}{4\bar{h}(1+\bar{h})+\bar{\sigma}}W_0^{*2}+1\right], & 0 \le W_0^* \le \frac{1}{1+2\bar{h}} \\ \frac{(1+2\bar{h})[(1+2\bar{h})(W_0^{*2}+1)+2(\bar{\sigma}-1)W_0^*]}{(1-\bar{a})[4\bar{h}(1+\bar{h})+\bar{\sigma}]}, & \frac{1}{1+2\bar{h}} \le W_0^* \le 1 \\ \frac{2(\bar{\sigma}+2\bar{h})(1+2\bar{h})}{(1-\bar{a})[4\bar{h}(1+\bar{h})+\bar{\sigma}]}W_0^*, & W_0^* \ge 1. \end{cases} \tag{3.9}$$

The external work will be dissipated by the overall deformation of the sandwich beam, and the absorbed plastic deformation energy U of the sandwich beam can be calculated as

$$U = \int_0^{W_0} P(W_0) dW_0. \tag{3.10}$$

From the above mentioned solutions and Eq. (3.10), one can easily calculate the dissipated plastic energy,

$$U^* = \begin{cases} \dfrac{1}{1-\bar{a}}\left[\dfrac{A_1\bar{\sigma}^2(1+2\bar{h})^2}{3(\bar{\sigma}+2\bar{h})^2}W_0^{*3} + W_0^*\right], \quad \text{for } 0 \le W_0^* \le \dfrac{(\bar{\sigma}+2\bar{h})n_2}{\bar{\sigma}(1+2\bar{h})} \\ \dfrac{1}{2(1-\bar{a})}\left[\dfrac{4A_1\bar{\sigma}^2(1+2\bar{h})^2}{3(\bar{\sigma}+2\bar{h})^2(\bar{\sigma}+1)}W_0^{*3} - \dfrac{4K_3A_1\bar{\sigma}^2(1+2\bar{h})^2}{(\bar{\sigma}+2\bar{h})^2(\bar{\sigma}+1)}W_0^{*2}\right] \\ \quad + \dfrac{1}{2(1-\bar{a})}\left[\dfrac{4K_1^2A_1\bar{\sigma}^2(1+2\bar{h})^2}{(\bar{\sigma}+2\bar{h})^2(\bar{\sigma}+1)} + C_1 + D_1 - A_1\bar{\sigma} + 1\right]W_0^* + K_3, \\ \qquad \text{for} \quad \dfrac{(\bar{\sigma}+2\bar{h})n_2}{\bar{\sigma}(1+2\bar{h})} \le W_0^* \le 1 - \dfrac{(\bar{\sigma}+2\bar{h})(1+n_1)}{1+2\bar{h}} \\ \dfrac{1}{1-\bar{a}}\left[\dfrac{A_1\bar{\sigma}(1+2\bar{h})^2}{3(\bar{\sigma}+2\bar{h})^2}W_0^{*3} + \dfrac{A_1\bar{\sigma}(1+2\bar{h})(\bar{\sigma}-1)}{(\bar{\sigma}+2\bar{h})^2}W_0^{*2} + \dfrac{A_1\bar{\sigma}(1+2\bar{h})^2}{(\bar{\sigma}+2\bar{h})^2}W_0^*\right] \\ \quad + K_4, \quad \text{for } 1 - \dfrac{(\bar{\sigma}+2\bar{h})(1+n_1)}{1+2\bar{h}} \le W_0^* \le 1 \\ \dfrac{A_1\bar{\sigma}(1+2\bar{h})}{(1-\bar{a})(\bar{\sigma}+2\bar{h})}W_0^{*2} + K_5, \quad \text{for } \; W_0^* \ge 1, \end{cases} \tag{3.11a}$$

for the case of $-1 \le \delta \le 0$, and

$$U^* = \begin{cases} \dfrac{1}{1-\bar{a}}\left[\dfrac{A_1\bar{\sigma}^2(1+2\bar{h})^2}{3(\bar{\sigma}+2\bar{h})^2}W_0^{*3} + W_0^*\right], \quad 0 \le W_0^* \le -\dfrac{(\bar{\sigma}+2\bar{h})n_1}{\bar{\sigma}(1+2\bar{h})} \\ \dfrac{1}{2(1-\bar{a})}\left[\dfrac{4A_1\bar{\sigma}^2(1+2\bar{h})^2}{3(\bar{\sigma}+2\bar{h})^2(\bar{\sigma}+1)}W_0^{*3} - \dfrac{4K_1A_1\bar{\sigma}^2(1+2\bar{h})^2}{(\bar{\sigma}+2\bar{h})^2(\bar{\sigma}+1)}W_0^{*2}\right] \\ \quad + \dfrac{1}{2(1-\bar{a})}\left[\dfrac{4K_2^2A_1\bar{\sigma}^2(1+2\bar{h})^2}{(\bar{\sigma}+2\bar{h})^2(\bar{\sigma}+1)} + B_1 - C_1 - A_1\bar{\sigma} + 1\right]W_0^* + K_6, \\ -\dfrac{(\bar{\sigma}+2\bar{h})n_1}{\bar{\sigma}(1+2\bar{h})} \le W_0^* \le 1 - \dfrac{(\bar{\sigma}+2\bar{h})(1-n_2)}{1+2\bar{h}} \\ \dfrac{1}{1-\bar{a}}\left[\dfrac{A_1\bar{\sigma}(1+2\bar{h})^2}{3(\bar{\sigma}+2\bar{h})^2}W_0^{*3} + \dfrac{A_1\bar{\sigma}(1+2\bar{h})(\bar{\sigma}-1)}{(\bar{\sigma}+2\bar{h})^2}W_0^{*2} + \dfrac{A_1\bar{\sigma}(1+2\bar{h})^2}{(\bar{\sigma}+2\bar{h})^2}W_0^*\right] \\ \quad + K_7, \quad 1 - \dfrac{(\bar{\sigma}+2\bar{h})(1-n_2)}{1+2\bar{h}} \le W_0^* \le 1 \\ \dfrac{A_1\bar{\sigma}(1+2\bar{h})}{(1-\bar{a})(\bar{\sigma}+2\bar{h})}W_0^{*2} + K_8, W_0^* \ge 1 \end{cases} \tag{3.11b}$$

for the case of $0 < \delta \leq 1$, in which

$$U^* = \frac{U}{P_c(c + h_t + h_b)}$$

$$K_3 = \frac{\begin{array}{c}(1+\alpha)^3\bar{\sigma}^3(7+\bar{\sigma}^2) + 6(1+\alpha)^2\bar{h}\bar{\sigma}^2[1+7\alpha+8\bar{\sigma}+(\alpha-1)\bar{\sigma}^2] \\ +12(1+\alpha)\bar{h}^2\bar{\sigma}[-5+2\alpha+7\alpha^2+16\alpha\bar{\sigma}+(13-2\alpha+\alpha^2)\bar{\sigma}^2]\end{array}}{\begin{array}{c}12(1-\bar{a})(\alpha+1)(1+2\bar{h})\bar{\sigma}(1+\bar{\sigma})\{4\bar{h}\bar{\sigma}(1+\alpha)^2+(1+\alpha)^2\bar{\sigma}^2 \\ +\bar{h}^2[-4(-1+\alpha)^2+8\bar{\sigma}(1+\alpha^2)]\}\end{array}}$$

$$+ \frac{\begin{array}{c}8\bar{h}^3[5-15\alpha+3\alpha^2+7\alpha^3+8(-1+3\alpha^2)\bar{\sigma}+(-5+39\alpha-3\alpha^2 \\ +\alpha^3)\bar{\sigma}^2+16\bar{\sigma}^3]\end{array}}{\begin{array}{c}12(1-\bar{a})(\alpha+1)(1+2\bar{h})\bar{\sigma}(1+\bar{\sigma})\{4\bar{h}\bar{\sigma}(1+\alpha)^2+(1+\alpha)^2\bar{\sigma}^2 \\ +\bar{h}^2[-4(-1+\alpha)^2+8\bar{\sigma}(1+\alpha^2)]\}\end{array}} l$$

$$K_4 = -\frac{\begin{array}{c}\bar{\sigma}^2(1+\alpha)^3(6\bar{h}+2-\bar{\sigma})+12(1+\alpha)\bar{h}^2\bar{\sigma}[(\alpha-1)^2+4\alpha\bar{\sigma}] \\ +8\bar{h}^3[(1-2\bar{\sigma})(-1+\alpha)^3+2\alpha(3+\alpha^2)\bar{\sigma}^2]\end{array}}{\begin{array}{c}3(1-\bar{a})(\alpha+1)(1+2\bar{h})\bar{\sigma}\{4\bar{h}\bar{\sigma}(1+\alpha)^2+(1+\alpha)^2\bar{\sigma}^2+\bar{h}^2[-4(-1+\alpha)^2 \\ +8\bar{\sigma}(1+\alpha^2)]\}\end{array}}$$

$$K_5 = \frac{\begin{array}{c}(1+\alpha)^3\bar{\sigma}^2(6\bar{h}+\bar{\sigma})+12(1+\alpha)\bar{h}^2\bar{\sigma}[-(\alpha-1)^2+2\bar{\sigma}(1+\alpha^2)] \\ +8\bar{h}^3[(-1+2\bar{\sigma})(-1+\alpha)^3+(2+6\alpha^2)\bar{\sigma}^2]\end{array}}{\begin{array}{c}3(1-\bar{a})(\alpha+1)(1+2\bar{h})\bar{\sigma}\{4\bar{h}\bar{\sigma}(1+\alpha)^2+(1+\alpha)^2\bar{\sigma}^2+\bar{h}^2[-4(-1+\alpha)^2 \\ +8\bar{\sigma}(1+\alpha^2)]\}\end{array}}$$

$$K_6 = \frac{[2(-1+\alpha)\bar{h}-(\alpha+1)\bar{\sigma}]^3(1+\bar{\sigma}-3\bar{\sigma}^2+\bar{\sigma}^3)}{\begin{array}{c}6(1-\bar{a})(\alpha+1)(1+2\bar{h})\bar{\sigma}(1+\bar{\sigma})\{4\bar{h}\bar{\sigma}(1+\alpha)^2+(1+\alpha)^2\bar{\sigma}^2 \\ +\bar{h}^2[-4(-1+\alpha)^2+8\bar{\sigma}(1+\alpha^2)]\}\end{array}}$$

$$K_7 = -\frac{\begin{array}{c}\bar{\sigma}^2(1+\alpha)^3(6\bar{h}+2-\bar{\sigma})+12(1+\alpha)\bar{h}^2\bar{\sigma}[(\alpha-1)^2+4\alpha\bar{\sigma}] \\ +8\bar{h}^3[(2\bar{\sigma}-1)(-1+\alpha)^3+(2+6\alpha^2)\bar{\sigma}^2]\end{array}}{\begin{array}{c}3(1-\bar{a})(\alpha+1)(1+2\bar{h})\bar{\sigma}\{4\bar{h}\bar{\sigma}(1+\alpha)^2+(1+\alpha)^2\bar{\sigma}^2+\bar{h}^2[-4(-1+\alpha)^2 \\ +8\bar{\sigma}(1+\alpha^2)]\}\end{array}}$$

$$K_8 = \frac{\begin{array}{c}\bar{\sigma}^2(1+\alpha)^3(6\bar{h}+\bar{\sigma})+12(1+\alpha)\bar{h}^2\bar{\sigma}[-(\alpha-1)^2+2\bar{\sigma}(1+\alpha^2)] \\ +8\bar{h}^3[(1-2\bar{\sigma})(-1+\alpha)^3+2\alpha(3+\alpha^2)\bar{\sigma}^2]\end{array}}{\begin{array}{c}3(1-\bar{a})(\alpha+1)(1+2\bar{h})\bar{\sigma}\{4\bar{h}\bar{\sigma}(1+\alpha)^2+(1+\alpha)^2\bar{\sigma}^2+\bar{h}^2[-4(-1+\alpha)^2 \\ +8\bar{\sigma}(1+\alpha^2)]\}\end{array}}$$

Let the asymmetric factor $\alpha = 1$, then Eqs. (3.11a) and (3.11b) reduce to the following solutions for symmetric sandwich beam transversely loaded by a flat punch at midspan [Qin and Wang, 2009a].

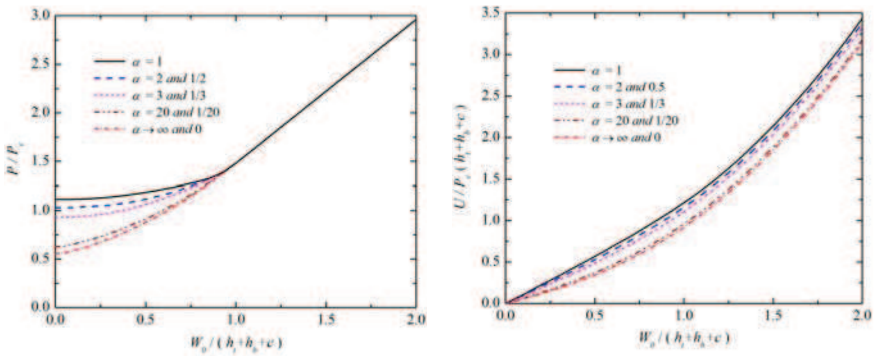

(a) (b)

Fig. 6. The effect of asymmetric factor on the load-carrying and energy absorption capacities of the fully clamped asymmetric metal sandwich beams with $\sigma_c/\sigma_f = 0.1$, $h/c = 0.1$ and $a/L = 0.1$: (a) load *vs* deflection and (b) energy *vs* deflection.

The solutions Eqs. (3.8a), (3.9) and (3.11a) are shown in Figs. 6(a) and 6(b), respectively. It is seen from Fig. 6(a) that the load-carrying capacities of the asymmetric sandwich beams decrease with the increase of α before deflection exceeds the depth of the sandwich beams as $\alpha > 1$. It is clear from Fig. 6(a) that the load-carrying capacities of the asymmetric sandwich beams are the same as that of symmetric one as the deflection exceeds the depth of the sandwich beams, while the difference of the plastic energy absorption among the asymmetric sandwich beams is almost a constant when the deflection exceeds the depth of the sandwich beams, as shown in Fig. 6(b). This may be due to the fact that the sandwich beams are in the membrane state and behave like a stretched plastic string as the deflection becomes large. For the case of $\alpha = 20$ or $\alpha = 1/20$, the load-carrying and energy absorption capacities of asymmetric sandwich beams are nearly equivalent to those as $\alpha \to \infty$ or $\alpha \to 0$. This means that the load-carrying and energy-carrying capacities of the symmetric sandwich beams are better than the asymmetric ones. For a fixed value of deflection, one can see from Fig. 6(a) that the predicted transition point between the end of plastic collapse with moment-axial force interaction and the start of membrane state occurs in the deflection of the depth, for the fully clamped asymmetric sandwich beam, which is the same as that of the symmetric sandwich beam [Qin and Wang, 2009a]. The stiffening induced by membrane forces becomes more clearly at large deflection, as shown in Fig. 6(a).

3.2. *The plastic neutral surfaces located out of the core ($\delta < -1$ and $\delta > 1$)*

According to the associated flow rules of yield criteria Eqs. (2.14a) and (2.14b) for asymmetric sandwich beam and similar to Sec. 3, we have

$$W_0^* = \frac{W_0}{c + h_t + h_b} = \begin{cases} \dfrac{\bar{\sigma} + 2\bar{h}}{1 + 2\bar{h}} n, & 0 \le n \le n_1 \\[2ex] \dfrac{(\bar{\sigma} + 2\bar{h})(1 + \bar{\sigma})}{2\bar{\sigma}(1 + 2\bar{h})} n + \dfrac{(\bar{\sigma} - 1)[2(\alpha - 1)\bar{h} - \bar{\sigma}(\alpha + 1)]}{2(\alpha + 1)\bar{\sigma}(1 + 2\bar{h})}, & n_1 \le n \le n_2 \\[2ex] \dfrac{\bar{\sigma} + 2\bar{h}}{1 + 2\bar{h}} n + \dfrac{1 - \bar{\sigma}}{1 + 2\bar{h}}, & n_2 \le n \le 1 \end{cases} \tag{3.12}$$

The relations between P/P_c and the normalized deflection W_0^* are

$$\frac{P}{P_c} = \begin{cases} \dfrac{1}{(1 - \bar{a})} \left[\dfrac{A_2(1 + 2\bar{h})^2}{(\bar{\sigma} + 2\bar{h})^2} W_0^{*2} + 1 \right], \quad 0 \le W_0^* \le \dfrac{(\bar{\sigma} + 2\bar{h}) n_1}{1 + 2\bar{h}} \\[2ex] \dfrac{1}{2(1 - \bar{a})} \left[\dfrac{4A_2\bar{\sigma}(1 + 2\bar{h})^2}{(\bar{\sigma} + 2\bar{h})^2(1 + \bar{\sigma})} W_0^{*2} - \dfrac{4B_2(1 + 2\bar{h})}{H_2(\bar{\sigma} + 1)} W_0^* \right. \\ \qquad \left. - \dfrac{B_2^2}{H_2(\bar{\sigma} + 1)(1 + \alpha)} + D_2 + 1 \right], \\ \dfrac{(\bar{\sigma} + 2\bar{h}) n_1}{1 + 2\bar{h}} \le W_0^* \le \dfrac{(\bar{\sigma} + 2\bar{h}) n_2 - \bar{\sigma} + 1}{1 + 2\bar{h}} \\[2ex] \dfrac{1}{2(1 - \bar{a})} \left[\dfrac{2A_2(1 + 2\bar{h})^2}{(\bar{\sigma} + 2\bar{h})^2} W_0^{*2} + \dfrac{6A_2(1 + 2\bar{h})(\bar{\sigma} - 1)}{(\bar{\sigma} + 2\bar{h})^2} W_0^* + \dfrac{2A_2(1 - \bar{\sigma})^2}{(\bar{\sigma} + 2\bar{h})^2} \right. \\ \qquad \left. + G_2 + F_2 + 1 \right], \dfrac{(\bar{\sigma} + 2\bar{h}) n_2 - \bar{\sigma} + 1}{1 + 2\bar{h}} \le W_0^* \le 1 \\[2ex] \dfrac{2A_2\bar{\sigma}(1 + 2\bar{h})}{(1 - \bar{a})(\bar{\sigma} + 2\bar{h})} W_0^*, \quad W_0^* \ge 1 \end{cases} \tag{3.13a}$$

and the relations of U^* and W_0^* are

$$U^* = \begin{cases} \dfrac{1}{(1-\bar{a})}\left[\dfrac{A_2(1+2\bar{h})^2}{3(\bar{\sigma}+2\bar{h})^2}W_0^{*3} + W_0^*\right], \quad 0 \le W_0^* \le \dfrac{(\bar{\sigma}+2\bar{h})n_1}{1+2\bar{h}} \\ \dfrac{1}{2(1-\bar{a})}\left\{\dfrac{4A_2\bar{\sigma}(1+2\bar{h})^2}{3(\bar{\sigma}+2\bar{h})^2(1+\bar{\sigma})}W_0^{*3} - \dfrac{2B_2(1+2\bar{h})}{H_2(\bar{\sigma}+1)}W_0^{*2} \right. \\ \quad \left. + \left[-\dfrac{B_2^2}{H_2(\bar{\sigma}+1)(1+\alpha)} + D_2 + 1\right]W_0^*\right\} + K_9, \\ \quad \dfrac{(\bar{\sigma}+2\bar{h})n_1}{1+2\bar{h}} \le W_0^* \le \dfrac{(\bar{\sigma}+2\bar{h})n_2 - \bar{\sigma}+1}{1+2\bar{h}} \\ \dfrac{1}{2(1-\bar{a})}\left\{\dfrac{2A_2(1+2\bar{h})^2}{3(\bar{\sigma}+2\bar{h})^2}W_0^{*3} + \dfrac{3A_2(1+2\bar{h})(\bar{\sigma}-1)}{(\bar{\sigma}+2\bar{h})^2}W_0^{*2} \right. \\ \quad \left. + \left[\dfrac{2A_2(1-\bar{\sigma})^2}{(\bar{\sigma}+2\bar{h})^2} + G_2 + F_2 + 1\right]W_0^*\right\} + K_{10}, \\ \quad \dfrac{(\bar{\sigma}+2\bar{h})n_2 - \bar{\sigma}+1}{1+2\bar{h}} \le W_0^* \le 1 \\ \dfrac{A_2\bar{\sigma}(1+2\bar{h})}{(1-\bar{a})(\bar{\sigma}+2\bar{h})}W_0^{*2} + K_{11}, W_0^* \ge 1 \end{cases} \tag{3.13b}$$

where

$$K_9 = \frac{[2\bar{h}(\alpha-1) - \bar{\sigma}(1+\alpha)]^3[1+2\bar{\sigma}^2 - 4\bar{\sigma}^3 + \bar{\sigma}^4]}{6(\alpha+1)^2(1+2\bar{h})\bar{\sigma}(1+\bar{\sigma})\{4\bar{h}^2(1+\alpha) - (1+\alpha)(-2+\bar{\sigma})\bar{\sigma} + 4\bar{h}[2+(-1+\alpha)\bar{\sigma}]\}}$$

$$K_{10} = \frac{2(\bar{\sigma}-1)[12\bar{h}^2(\alpha-1)^2 - 6\bar{h}(\alpha^2-1)(\bar{\sigma}-1) + (1+\alpha)^2(2-3\bar{\sigma}+2\bar{\sigma}^2)]}{3(\alpha+1)(1+2\bar{h})\{4\bar{h}^2(1+\alpha) - (1+\alpha)(-2+\bar{\sigma})\bar{\sigma} + 4\bar{h}[2+(-1+\alpha)\bar{\sigma}]\}}$$

$$K_{11} = \frac{2\{8\bar{h}^3(\alpha+1)^2 + 12\bar{h}^2[4\alpha + (-1+\alpha)^2\bar{\sigma}] + (1+\alpha)^2\bar{\sigma}(2-2\bar{\sigma}+\bar{\sigma}^2) - 6\bar{h}[-2(1+\alpha) + (-1+\alpha^2)\bar{\sigma}(\bar{\sigma}-2)]\}}{3(\alpha+1)(1+2\bar{h})\{4\bar{h}^2(1+\alpha) - (1+\alpha)(-2+\bar{\sigma})\bar{\sigma} + 4\bar{h}[2+(-1+\alpha)\bar{\sigma}]\}}$$

Replacing α and m in Eqs. (3.13a) and (3.11b) by $1/\alpha$ and $-m$, we can obtain the solutions for the case of plastic neutral surface in the bottom face sheet.

4. Numerical Solutions and Discussions

Finite element calculations are carried out herein to study the large deflection of a fully clamped asymmetric metal foam core sandwich beams under transverse loading. The displacement loading is applied to a rigid roller. ABAQUS/Standard code is employed, and four node and bilinear plane strain quadrilateral elements (Type CPE4) with full integration are selected to model both the foam core and the face sheets. Due to the symmetry of the problem, half of the sandwich beam is considered in calculations. The vertical, horizontal and rotational displacements of nodes at the ends of the beam are zero. The contact property between the outer surface of the top face sheet and the rigid roller is modeled as frictionless as provided in ABAQUS code The typical samples of the asymmetric sandwich beams are considered as follows.

The half span of the sandwich beam is $L = 1500\,\text{mm}$, the height of the foam core and total thicknesses of the top and bottom face sheets are $c = 50\,\text{mm}$ and $h_t + h_b = 10\,\text{mm}$. Thus, $\bar{c} = 0.0333$ and $\bar{h} = 0.1$, respectively. Radius of the loading roller is $R = 4\,\text{mm}$, then $\bar{R} = R/L = 0.00267$. Four kinds of the asymmetric factor are considered: 1) $\alpha = 2$, 2) $\alpha = 1/2$. There are 4500 elements in the computational model Appropriate mesh refinement at the location of loading point and near the end support of the sandwich beam is included and mesh sensitivity is checked in calculations.

The face sheets obey J_2 flow theory of plasticity. The metal foam obeys Deshpande-Fleck constitutive model [Deshpande and Fleck, 2000] implemented in ABAQUS which allows the shape change of yield surface due to differential hardening along the hydrostatic and deviatoric axes. The yield function for the foam core is

$$\psi = \hat{\sigma} - \sigma_c = 0, \tag{4.1}$$

where

$$\hat{\sigma}^2 \equiv \frac{1}{1 + (\gamma/3)^2}(\sigma_e^2 + \sigma_m^2), \tag{4.2}$$

with $\sigma_e \equiv \sqrt{3s_{ij}s_{ij}/2}$ being von Mises effective stress, s_{ij} the deviatoric stress, $\sigma_m \equiv \sigma_{kk}/3$ the mean stress and γ the shape factor of yield surface. The associated plastic flow rule is adopted and the plastic Poisson's v_p is calculated by

$$\nu_p = -\frac{\dot{\varepsilon}_{22}^p}{\dot{\varepsilon}_{11}^p} = \frac{1/2-(\gamma/3)^2}{1 + (\gamma/3)^2}. \tag{4.3}$$

The top and bottom face sheets are aluminum with yield strength $\sigma_f = 30\,\text{MPa}$, Young's modulus $E_f = 70\text{GPa}$ and elastic Poisson's ratio $\nu_{ef} = 0.3$, respectively. It is assumed that the face sheet obeys linear hardening law with tangent modulus $E_{tf} = 5 \times 10^{-4}E_f$ and has sufficient ductility to sustain deformation without fracture. The isotropic aluminum foam core has yield strength $\sigma_c = 3\,\text{MPa}$ Young's modulus $E_{ef} = 1\,\text{GPa}$, and elastic Poisson's ratio $\nu_{ec} = 0.3$ and plastic Poission's ratio $\nu_p = 0$, respectively. The platform stress is σ_c and the densification strain $\varepsilon_D = 0.5$. Beyond densification, we assume that the metal foam obeys linear hardening law with tangent modulus $E_{ct} = 0.2E_f$.

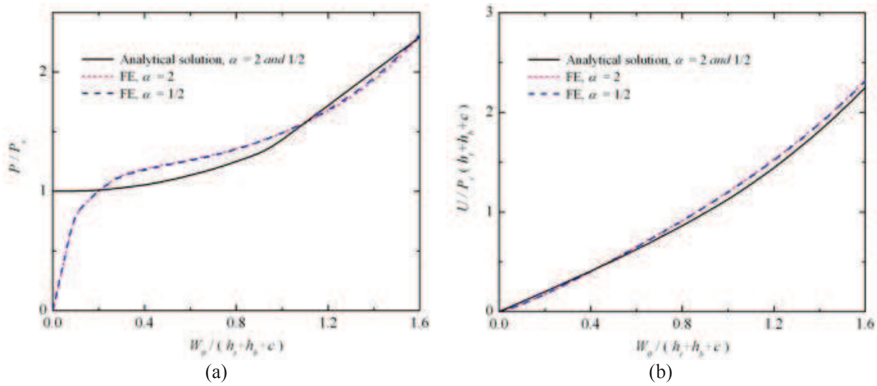

Fig. 7. Analytical and numerical solutions for the fully clamped asymmetric metal sandwich beams with a metal foam core with $\alpha = 2$ and $1/2$. (a) Load *vs* deflection and (b) energy *vs* deflection.

4.1. *Comparisons with analytical solutions*

In order to estimate the effect of strain hardening of face sheets, mean plastic flow stress $(\sigma_f + \sigma_u)/2$ (the ultimate tensile strength $\sigma_u = 47.5\,\text{MPa}$ and the rupture strain $\varepsilon_u = 50\%$ for face sheets) is used in theoretical analysis. Moreover, the length of the punch is $a \to 0$. Comparisons of the present analytical solutions and numerical results for $\alpha = 2$ and $1/2$ are shown in Fig. 7, respectively. It is seen that the present analytical solutions are in good agreement with numerical results in the post yield regime for the cases of $\alpha = 2$ and $\alpha = 1/2$ whose plastic neutral surfaces locate in the core, as shown in Figs. 7(a) and 7(b). The discrepancy appeared in the case of the small deflection may be due to neglecting the elastic deformation in theoretical analysis. Also, it is shown that the present analytical solutions for energy-deflection relation are in excellent agreement with numerical results, as shown in Fig. 7(b).

4.2. *Deformation mechanisms*

It is clear from Sec. 3 that large deflection of asymmetric metal foam core sandwich beams involves two phases, i.e. interaction of bending and axial stretching and membrane. When the initial plastic collapse has been attained, the interaction of bending moment and axial force should be considered as the maximum deflection approaches the cross-section depth $(h_t + h_b + c)$. If the deflection exceeds the depth of the sandwich cross-section, the membrane phase occurs. It is seen from Eq. (3.8c) and the fourth formula of Eq. (3.13a) that the sandwich beam stretches in a manner of plastic string and the load increases linearly with increasing the deflection.

Usually, it is difficult to give a general failure criterion for sandwich beam due to the fact that plastic strain distribution in the sandwich beam is sensitive to the initial collapse mechanism and support condition. Herein, neglecting the plastic strain due to bending, we state a simple failure criterion on the basis of critical tensile strain $_f$ of the face sheet induced by stretching. Thus, one can obtain the critical deflection W_f at failure,

$$W_{0f} \approx L\sqrt{2(1-\bar{a})\varepsilon_f} \tag{4.4}$$

From Eq. (3.8c) and the fourth formula of Eq. (3.13a), we can respectively obtain the critical failure loads P_f for the asymmetric sandwich beam,

$$\frac{P_f}{P_c} = \frac{2A_1\bar{\sigma}}{\bar{c}(\bar{\sigma}+2\bar{h})}\sqrt{\frac{2\varepsilon_f}{1-\bar{a}}} \tag{4.5}$$

for the case of $-1 < \delta < 1$, and

$$\frac{P_f}{P_c} = \frac{2A_2\bar{\sigma}}{\bar{c}(\bar{\sigma}+2\bar{h})}\sqrt{\frac{2\varepsilon_f}{1-\bar{a}}} \tag{4.6}$$

for the case of $\delta > 1$, where $\bar{c} = c/L$

4.3. *The effects of core strength and loading punch size*

The effects of core strength and loading punch size on the relation of load versus deflection for the fully clamped asymmetric (e.g., $\alpha = 2$) sandwich beam under transverse loading by a flat punch are shown in Figs. 8 and 9, respectively. It is readily seen that the core strength and loading punch size have significant effect on the load-carrying of asymmetric metal sandwich structure. For a fixed value of deflection, the load increases with the increase of core strength and loading punch size, which become more significant in the case of large deflection. It is obvious from Eqs. (3.11a) and (3.11b) that for a fixed value of the plastic energy, the smaller the core strength and loading punch sizes are, the larger the corresponding deflection of the sandwich beam are.

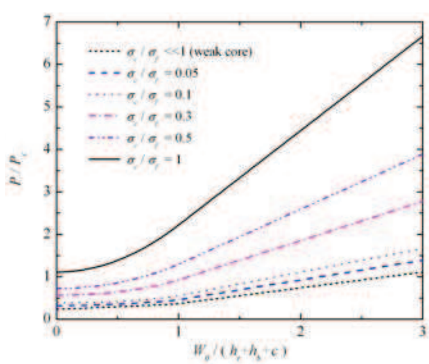

Fig. 8. The effect of core strength on the load-carrying of fully clamped asymmetric metal sandwich beams with $a/L = 0.1$, $h/c = 0.1$ and $\alpha = 2$.

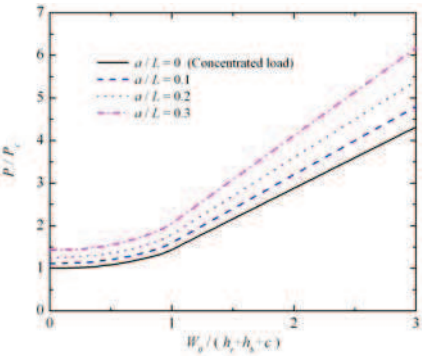

Fig. 9. The effect of the size of loading punch on the load-carrying of the fully clamped asymmetric sandwich beams with $\sigma_c/\sigma_f = 0.1$, $h/c = 0.1$ and $\alpha = 2$.

5. Conclusions

Large deflection of geometrically asymmetric metal foam core sandwich beam was analytically and numerically studied under transversely loading by a flat punch. A yield criterion was proposed for geometrically asymmetric sandwich structures, and analytical solution was obtained for the large deflection of fully clamped slender asymmetric sandwich beam, in which the interaction of bending and axial stretching was considered. The present analytical solution agrees well with the finite element numerical results. It can be concluded that the core strength and loading punch size have significant effects on the structural response of geometrically asymmetric sandwich beam, and the effect of asymmetry is negligible as the deflection is larger than the depth of the sandwich beam. It is clear that the axial stretching induced by large deflection should be considered in large deflection analysis, which plays an important role in the post-yield regime. Also, the present method is efficient and simple to deal with large deflection problem of asymmetric metal sandwich structure

Acknowledgments

This work was supported by NSFC (11021202, 11102146) and the Fundamental Research Funds for the Central Universities.

References

Ashby, M. F., Evans, A. G., Fleck, N. A., Gibson, L. J., Hutchinsion, J. W., Wadley and H. N. G. [2000] "*Metal Foams: A Design Guide*". Butterworth Heinemann, Oxford.

Bart-Smith, H., Hutchinson, J. W. and Evans, A. G. [2001] "Measurement and analysis of the structural performance of cellular metal sandwich construction." *International Journal of Mechanical Sciences* **43**, 1945–1963.

Bart-Smith, H., Hutchinson, J. W., Fleck, N. A. and Evans, A. G. [2002] "Influence of imperfections on the performance of metal foam core sandwich panels." *International Journal of Solids and Structures* **39**, 4999–5012.

Deshpande, V. S. and Fleck, N.A. [2000] "Isotropic constitutive models for metallic foams." *Journal of the Mechanics and Physics of Solids* **48**, 1253–1283.

Deshpande, V. S. and Fleck, N. A. [2001] "Collapse of truss core sandwich beams in 3-point bending." *International Journal of Solids and Structures* **38**, 6275–6305.

Deshpande, V. S. and Fleck, N. A. [2003] "Energy absorption of an egg-box material." *Journal of the Mechanics and Physics of Solids* **51**, 187–208.

Fleck, N. A. and Deshpande, V. S. [2004] "The resistance of clamped sandwich beams to shock loading." *ASME, Journal of Applied Mechanics* **71**, 386–401.

Frostig, Y., Baruch, M., Vilnay, O. and Sheinman, I. [1991] "Bending of nonsymmetric sandwich beams with transversely flexible core." *ASCE, Journal of Engineering Mechanics* **117**, 1931–1952.

Gibson, L. J. and Ashby, M. F. [1997] "Cellular Solids: Structure and Properties" 2nd edn. Cambridge University Press, Cambridge.

Haythornwaite, R. M. [1957] "Beams with full end fixity." *Engineering* **183**, 110–112.

Martin, J. B. [1975]. Plasticity: Fundamentals and General Results. The MIT Press, Cambridge, Mass.

McCormack, T. M., Miller, R., Kesler, O. and Gibson, L. J. [2001] "Failure of sandwich beams with metallic foam cores." *International Journal of Solids and Structures* **38**, 4901–4920.

Noor, A. K., Burton, W. S. and Bert, C. W. [1996] "Computational models for sandwich panels and shells." *Applied Mechanics Reviews* **49**, 155–199.

Onat, E. T. and Prager, W. [1953] "Limit analysis of arches." *Journal of the mechanics and physics of solids* **1**, 77–89.

Qin, Q. H. and Wang, T. J. [2007] "Impulsive loading of a fully clamped circular metallic foam core sandwich plate," *Proceedings of the Seventh International Conference on Shock and Impact Loads on Structures*. (CIPREMIER PTE LTD, Beijing, China), pp. 481–488.

Qin, Q. H. and Wang, T. J. [2008] "Analytical solution for the large deflection of fully clamped metallic foam sandwich beam." *Advanced Materials Research* **33–37**, 559–565.

Qin, Q. H., Wang, T. J. [2009a] "An analytical solution for the large deflections of a slender sandwich beam with a metallic foam core under transverse loading by a flat punch." *Composite Structures* **88**, 509–518.

Qin, Q. H. and Wang, T. J. [2009b] "A theoretical analysis of the dynamic response of metallic sandwich beam under impulsive loading." *European Journal of Mechanics — A/Solids* **28**, 1014–1025.

Qin, Q. H. and Wang, T. J. [2011] "Low-velocity heavy-mass impact response of slender metal foam core sandwich beam." *Composite Structures* **93**, 1526–1537.

Qin, Q. H., Wang, T. J. and Zhao, S. Z. [2009] "Large deflections of metallic sandwich and monolithic beams under locally impulsive loading." *International Journal of Mechanical Sciences* **51**, 752–773.

Queheillalt, D. T. and Wadley, H. N. G. [2005] "Pyramidal lattice truss structures with hollow trusses." *Materials Science and Engineering A* **397**, 132–137.

Romanoff, J. and Varsta, P. [2006] "Bending response of web-core sandwich beams." *Composite Structures* **73**, 478–487.

Russell, B. P., Liu, T., Fleck, N. A. and Deshpande, V. S. [2011] "Quasi-static three-point bending of carbon fiber sandwich beams with square honeycomb cores." *Journal of Applied Mechanics* **78**, 031008–031015.

Sypeck, D. J. and Wadley, H. N. G. [2001] "Multifunctional microtruss laminates: textil synthesis and properties." *Journal of Materials Research* **16**, 890–897.

Tagarielli, V. L. and Fleck, N. A. [2005] "A comparison of the structural response of clamped and simply supported sandwich beams with aluminium faces and a metal foam core." *ASME*, *Journal of Applied Mechanics* **72**, 408–417.

Tagarielli, V. L., Fleck, N. A. and Deshpande, V. S. [2004] "Collapse of clamped and simply supported composite sandwich beams in three-point bending." *Composites Part B-Engineering* **35**, 523–534.

Wadley, H. N. G., Fleck, N. A. and Evans, A. G. [2003] "Fabrication and structural performance of periodic cellular metal sandwich structures." *Composites Science and Technology* **63**, 2331–2343.

Xu, Z. M., Zhang, W. X. and Wang, T. J. [2010] "Deformation of closed-cell foams incorporating the effect of inner gas pressure." *International Journal Applied Mechanics* **2**, 489–513.